JOTCS
Journal of the Turkish Chemical Society
Section: A
Chemistry
TURKISH CHEMICAL SOCIETY

Structural, Optical, and Morphological Characterization of Silica Nanoparticles Prepared by Sol-Gel Process

Most. Nilufa Yeasmin[1*], Munira Sultana[1], Ayesha Siddika[1], Samia Tabassum[1], Saeed Mahmud Ullah[2], Muhammad Shahriar Bashar[1]

[1]Institute of Fuel Research and Development, Bangladesh Council of Scientific and Industrial Research, Dhaka, 1205, Bangladesh

[2]University of Dhaka, Department of Electrical and Electronic Engineering, Dhaka, 1000, Bangladesh

*Corresponding author's e-mail: nilufayeasmin205@gmail.com

Abstract: In the current years, silica nanoparticles have become more favorable in various disciplines such as medicine, nano-biotechnology, the food industry, and drug delivery due to their tunable physicochemical characteristics. In this paper, the silica nanoparticles were synthesized by hydrolysis and condensation of tetra-ethyl-ortho-silicate (TEOS) in an ethanolic medium using ammonia as a stimulator in the reaction. The chemical bond structures of silica nanoparticles were analyzed by Fourier Transform Infrared Spectroscopy (FT-IR) which confirmed the existence of the Si-O bonds according to the different absorption peaks of the samples. The amorphous structure of these nanoparticles was certified by finding the board peaks in the X-Ray Diffraction (XRD) patterns. The elemental chemical composition of silica nanoparticles was investigated by Energy Dispersive X-Ray Spectroscopy (EDX) where 61.48wt % of silicon and 23.48wt% of oxygen were found. Almost round-shaped spherical and uniform silica nanoparticles with smooth surfaces were investigated by Scanning Electron Microscopy (SEM) measurement. The different particle sizes of silica nanoparticles within the range of 95 ± 5.59 to 280 ± 7.8 nm were found by controlling the concentration of TEOS. The optical absorption spectra and band gap calculations were also analyzed by Ultraviolet-Visible (UV-Vis) spectrophotometry for the different concentrations of TEOS. The results revealed that with increasing the concentration of TEOS, the absorption spectra of silica nanoparticles increased and their optical bandgap decreased from 3.92 eV to 3.79 eV.

Keywords: Silica nanoparticles, TEOS, sol-gel process, amorphous, spherical.

INTRODUCTION

Nowadays research on nano-materials has drawn great attention to the scientific community for their size-dependent appealing characteristics at the nano-scale (1–3). In recent years, colloidal silica nano-spheres have been caught up a prominent position across various scientific disciplines due to their huge industrial demands and different potential applications as biosensors, thin films, catalysis, nano-glass, nano-filler, ceramics, stabilizers, electronic substrates, photonic crystal, electrical/thermal insulators, emulsifiers, binder, pigments, and semiconductor adsorbents (4–9). Due to their high surface area, non-toxicity, controlled particle size, and high functionality, they are also widely used in the DNA-conjugation, food industry, drug delivery, and as a doping material in various nanotech industries (1,10). To ensure the quality of these products, narrow particle size and uniform distribution of silica nanoparticles are a great concern in this case (11).

There are mainly two distinct approaches to producing silica nanoparticles; one is the physical synthesis and another is the chemical synthesis approach. As these nanoparticles need more development due to their high purity and narrow size distribution so, the chemical synthesis method is more efficient than the physical synthesis method (10,12). However, this widely used chemical synthesis approach can be further classified as the fumed (pyrogenic) synthesis, the micro emulsion-gel synthesis, and the sol-gel synthesis process. Again, the sol-gel synthesis process can be categorized as precipitated synthesis, stöber method synthesis, and biomimetic sol-gel synthesis process (13,14).

Firstly, in the pyrogenic synthesis process, silicon tetrachloride ($SiCl_4$) is used to produce silica nanoparticles by combustion at a temperature of 100 °C. This process, however, is not industrially feasible for the difficulty to control their particle sizes and morphology (13–15). Then, in the micro-emulsion gel process, highly stabilized nanoparticles are yielded from the homogenous mixture of water, oil, and surfactant medium. Though this procedure is very efficient for producing ultrafine silica nanoparticles, it is not industrially cost-effective (16,17). Among those processes, the highly reactive, spherical, and industrially suitable nano-silica can be easily synthesized through the sol-gel process. Because, this process offers many benefits over other processes, due to its simplicity and flexibility by changing the different parameters during synthesis (18,19).

However, silica nanoparticles can be extracted from various natural sources such as rice husk, sugarcane bagasse, corn cob, wheat husk, coffee husk, and also other agricultural wastes. Since extracted silica nanoparticles from these biomass sources contain a large amount of

metal and non-metal impurities, so they aren't favorable for advanced industrial applications (1,20). For example, Zaky et al. produced silica nanoparticles with an average size of 50-70 nm from rice straw. These produced particles are agglomerated which limits their usage for industrial applications (21). For this reason, tetra-ethyl-ortho-silicate (TEOS) or tetra-methyl-ortho-silicate (TMOS) is used as a precursor during synthesis for commercial applications. In addition, we also used ~~tetraethyl- ortho-silicate (TEOS)~~ TEOS as a silicon source to get spherical and uniform silica nanoparticles.

In 1968, Stöber et al. as a pioneer of this work, first synthesized silica nanoparticles through the sol-gel process where the hydrolysis and condensation of ~~tetraethyl- ortho-silicate (TEOS)~~ TEOS occurred under the catalytic influence of ammonia in an ethanolic medium. They obtained quasi-monodisperse silica nanoparticles with particle sizes of 0.5-2 μm by varying the concentration of precursor and using the different alcohol media as solvents (22). From the author's point of view, the morphology of particles and their size distribution with different degrees of dispersity can be strongly affected by the five key parameters such as the concentration of precursor (TEOS), catalyst, water, solvent (alcohols), and the reaction temperature (23–25). By controlling these variables, Rao et al. produced monodisperse and spherical silica nanoparticles with sizes ranging from 20 to 460 nm(26). Typical amorphous silica nanoparticles with different degrees of dispersity and particle size compared with other previous studies are summarized in Table 1.

Table 1: The comparison of average particle size, dispersity, and morphology of silica nanoparticles with the previous studies[1].

Synthesis process	Silicon source	Catalyst	Optimum Average particle size	Dispersity	Ref.
Sol-gel method	TEOS	NH_4OH	95 nm	Quasi-monodisperse	Present study
Sol-gel method	TEOS	NH_3	9 nm	Disperse	(27)
Sol-gel method	TEOS	PVP	25 nm	Monodisperse	(19)
Sol-gel method	TEOS	NH_3	7.1 nm	Disperse	(28)
Sol-gel Method	TEOS	$N(CH_2OH)_3$	42 nm	Aggregate	(29)
Microemulsion	TMOS	NH_3	11 nm	Aggregate	(16)

[1] The morphology is spherical in all instances.

Furthermore, the size and shape morphology of silica nanoparticles can be controlled by adding different kinds of electrolytes such as sodium iodide (NaI), ammonium bromide (NH_4Br), and also various types of surfactants such as cetyltrimethylammonium bromide (CTAB), polyvinyl pyrrolidone (PVP), sodium dodecyl sulphate (SDS) respectively (27,30,31). For example, Kim et al. have reported spherical and very fine silica nanoparticles by adding a slight amount of different electrolytes during synthesis (32). Similarly, R. Stanley and his coworkers have also prepared silica nanoparticles with the use of various surfactants by wet chemical synthesis route (15). Moreover, Guo et al. found the dispersed spherical, and amorphous silica nanoparticles with average particle sizes ranging from 13 to 32 nm by the modified Stöber synthesis method with a slow hydrolysis catalyst in water (33).

In our present work, quasi-monodisperse, spherical, and amorphous silica nanoparticles were fabricated via the sol-gel synthesis process using TEOS as a precursor and ammonia as a catalyst. In the sol-gel process, the concentration of TEOS is one of the most important controlling tools to get desired particle size and dispersity of silica nanoparticles. So, the uniform nanoparticles within a range of 95±5.59 ~ 280±7.8 nm in diameter were also reported in this paper by conducting the reaction at various concentrations of TEOS. After successfully synthesizing the silica nanoparticles, they were characterized by Scanning Electron Microscopy (SEM), Energy Dispersive X-Ray Spectroscopy (EDX), X-Ray Diffraction Spectroscopy (XRD), Fourier transform infrared spectroscopy (FT-IR), and Ultraviolet-Visible (UV-Vis) spectroscopy techniques.

EXPERIMENTAL SECTION

Materials

For the synthesis of silica nanoparticles, the chemicals such as Tetraethyl Ortho-silicate (TEOS, 99% GC), absolute ethanol (C_2H_5OH, 99.9%), and ammonium hydroxide (NH_4OH, 30%) were received from Sigma Aldrich and Merck Company Ltd respectively. All reagents and laboratory-produced distilled water were used without further purification.

Synthesis of Silica Nanoparticles

The most generalized reaction to form silica nanoparticles through the hydrolysis and poly-condensation of silicon alkoxides $(Si(OR)_4)$ can be expressed as (19):

$$\mathbf{Si(OR)_4 + H_2O \overset{Hydrolysis}{\Longleftrightarrow} Si(OH)_4 + 4ROH}$$

$$\mathbf{\equiv Si - OH + OH - Si \equiv \xrightarrow{Aqueous\ Condensation} \equiv Si - O - Si \equiv + H_2O}$$

$$\equiv \mathbf{Si} - \mathbf{OR} + \mathbf{OH} - \mathbf{Si} \equiv \xrightarrow{\textbf{Alcoholic Condensation}} \equiv \mathbf{Si} - \mathbf{O} - \mathbf{Si} \equiv \ + \mathbf{ROH}$$

The quasi-mono-disperse and spherical silica nanoparticles were synthesized from the sol-gel process through the hydrolysis and condensation reaction of TEOS. The whole procedure is schematically described in Figure 1. The amounts of precursor, solvent, and catalyst used in this experiment are also summarized in Table 2. The reaction was carried out in a 150 mL beaker where 30 mL of ethanol and 5 mL of distilled water were taken at first. The mixture of both ethanol and water was then stirred vigorously at 460 rpm at 55 °C temperature using a magnetic stirrer. After 10 minutes, TEOS was added drop-wise using an adjustable micropipette into the solution and agitated for the next 2 hours. Subsequently, ammonium hydroxide as a catalyst was added to keep up the expected alkalinity of the solution. The pH of the solution was measured by pH meter and recorded at pH=11-12 level (34). This transparent solution was then constantly agitated for the next 5 hours. Here, the volume of TEOS was varied to control the particle size and dispersity of silica nanoparticles where the other chemicals were kept at a fixed level. However, after adding the catalyst, the solution was finally turned into bluish milky white color. Then, the sol was centrifuged at 5000 rpm for 10 minutes, and separated the silica nanoparticles by washing with ethanol for three times to remove unreacted chemicals.

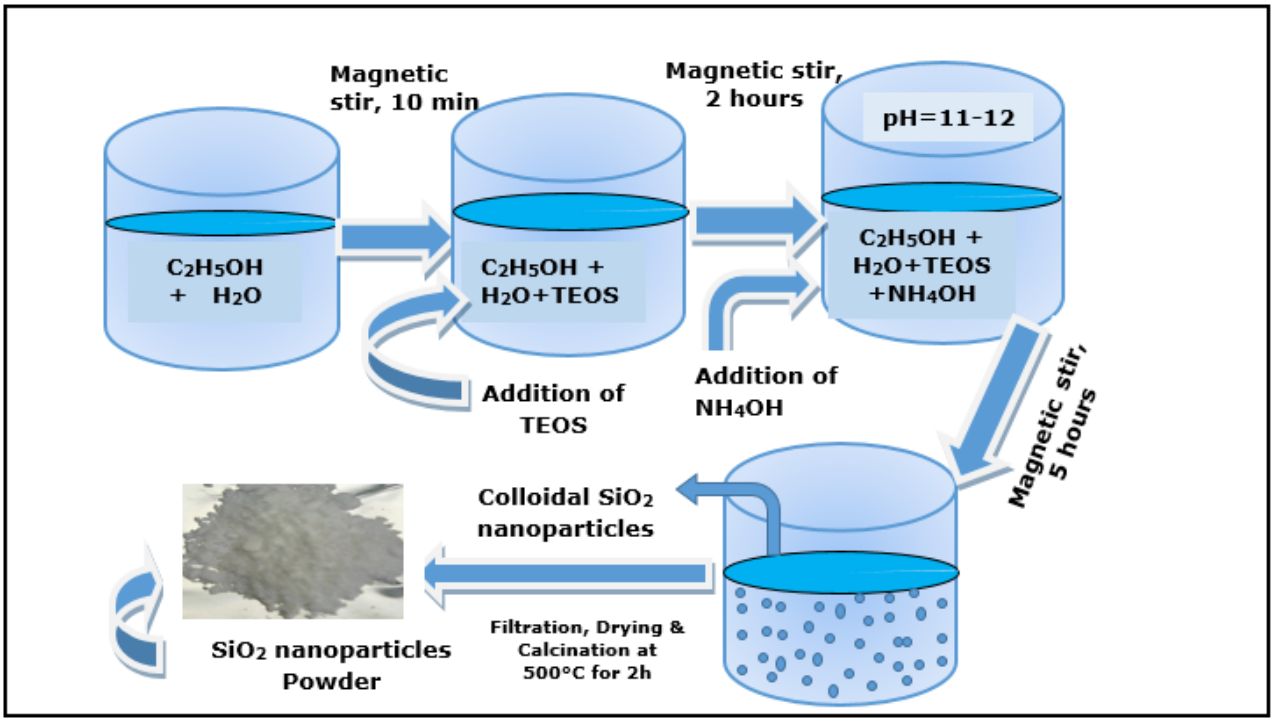

Figure 1: Schematic diagram of silica nanoparticles synthesis from the sol-gel process.

Table 2: Different amounts of chemicals used in this experiment.

Sample no.	Amount of TEOS (mL)	Average Particle Size, D(nm)
S1	1	95±5.6
S2	2	175±10.5
S3	3	280±7.8

In the experiments, 2 mL of NH_4OH, 30 mL of C_2H_5OH, and 5 mL of distilled H_2O were used.

The washed particles were then collected and dried at 70 °C for 24 hours. After oven-drying, the silica nanoparticles were calcined at 500 $^{\circ}$C for 2 hours and finally kept in a desiccator for further preservation.

Characterizations

The surface morphology, particle size, and shape of the silica nanoparticles were inspected by Scanning Electron Microscope (SEM, EVO-18, Carl Zeiss, Germany). The XRD patterns of these particles were obtained from GBC Emma X-ray Diffraction Spectroscopy that was equipped with the monochromatic Cu kαX-rays detector (λ=1.5206A^0 at 35.5 KV and 28mA). As a great tool for chemical bond identification, Fourier-transform infrared (FT-IR) spectroscopy (IR Tracer-100, Shimadzu, Japan) was conducted at a frequency range of 400-4000 cm^{-1}. The chemical composition of silica nanoparticles was analyzed by Energy Dispersive X-ray Spectroscopy (EDX) equipped with a Scanning Electron Microscope (SEM, JEOL/EO, Japan). The UV-Vis absorbance spectra were also recorded within the wavelength range of 300 to 1100 nm by Ultraviolet-Visible (UV-Vis) spectroscopy using a UH4150 (Hitachi, Japan) Spectrophotometer.

RESULTS AND DISCUSSION

Fourier-transform infrared spectroscopy (FT-IR) Analysis

To investigate the chemical bonds of the synthesized silica nanoparticles within the range 400-4000 cm^{-1}, FT-IR spectrum analysis was applied to the samples. The FTIR spectra for three different samples prepared using different amounts of TEOS and calcination at 500 °C for 2 hours are shown in Figure 2.

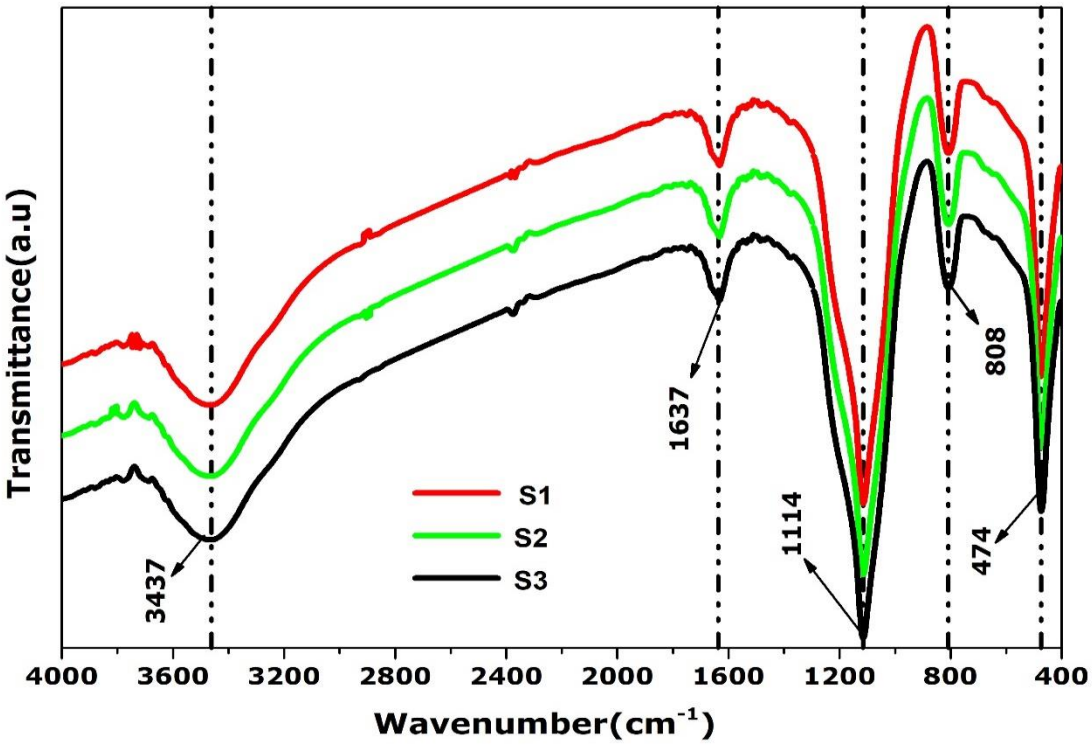

Figure 2: FT-IR spectra of silica nanoparticles prepared using different volume ratios of TEOS: water: Ammonia = **(S1)** 1:5:2 **(S2)** 1:2.5:1 **(S3)** 1.5:2.5:1 respectively.

The absorption peaks in FTIR spectra originated due to the different vibrations of chemical bonds of silica nanoparticles are described in **Table 3**. In FTIR spectra, the absorption peaks of the S1 sample indicate the silica nanoparticles which are produced from 1 mL of TEOS. For the S1 sample, the broad absorption peak at 3437 cm^{-1} is assigned to the stretching vibration of structural water -OH. A slightly intense absorption peak at 1637 cm^{-1} is attributed to the bending vibration of O-H due to the trapped water molecules inside the sample (27,35,36). This water was physically absorbed by the sample from the air after calcination. So, to prevent the absorption of water, the silica nanoparticles are recommended to keep in a moisture-free environment.

Table 3: Summary of common absorption peaks in FTIR analysis of the synthesized silica nanoparticles.

Serial No.	Absorption peak (cm^{-1})	Bond identification	References
1	474	-Si-O- bending vibration	(8,27,35,36)
2	808	-Si-O- symmetric stretching vibration	(8,27,35,36)
3	1114	-Si-O- asymmetric stretching vibration	(8,27,35,36)
4	1637	-O-H bending vibration due to trapped water molecules	(8,29,33,36)
5	3437	-O-H stretching vibration	(8,29,33,36)

However, the dominant absorption peaks in the S1 sample at 474, 808, and 1114 cm^{-1} are attributed to the stretching and bending vibrations of Si-O-Si (33,35,36). Furthermore, the sharp absorption peak at 1114 cm^{-1} is ascribed to the asymmetric stretching vibration of Si-O-Si while the absorption peak at 808 cm^{-1} and 474 cm^{-1} are expressed the relation to the symmetric stretching vibrations and bending vibrations of Si-O respectively (36,37). The FT-IR spectra in Figure 2 of S2 and S3 samples produced from the precursor using 2 mL and 3 mL of TEOS respectively show similar absorption peaks. Three dominant absorption peaks at 474, 808, and 1114 cm^{-1} related to the bending, symmetric and asymmetric vibrations of Si-O-Si respectively are found clearly in the three samples. Furthermore, the board absorption peak at 3437 cm^{-1} confirms the existence of the –OH group in all samples (8,29,33,36). Finally, The FT-IR spectra indicate that there are no significant differences in chemical structures among all the synthesized samples. However, these findings are consistent with the observations reported by Guo et al (33). He found almost similar absorption peaks in FT-IR spectra using different types of catalysts to produce spherical silica nanoparticles with uniform size distribution.

X-Ray Diffraction (XRD) Analysis

Figure 3 shows the XRD patterns of all samples of the silica nanoparticles to check the crystalline structures which were synthesized using different amounts of TEOS. From Figure 3, it has been shown that the XRD patterns of all the samples exhibit only broad diffused peaks around the region of $2\theta=24.58^0$ and there are no sharp diffraction peaks corresponding to any crystalline structures (19,33,36). However, these broad diffraction peaks correspond that all the samples

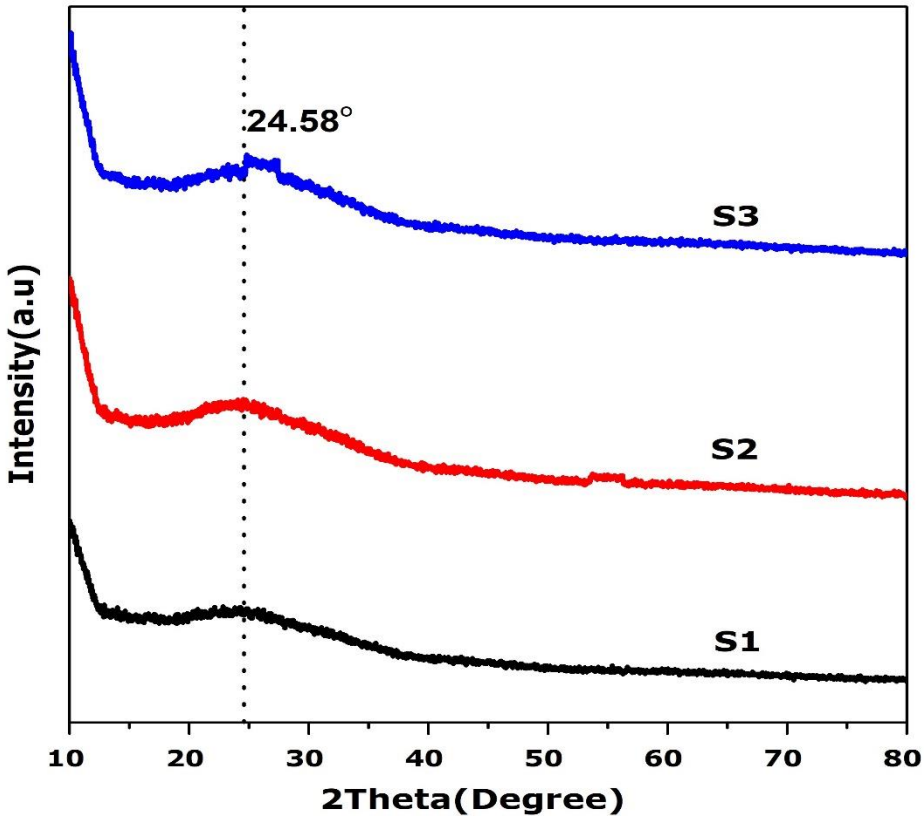

Figure 3: XRD patterns of the silica nanoparticles prepared using different volume ratios of TEOS: water: Ammonia = **(S1)** 1:5:2 **(S2)** 1:2.5:1 **(S3)** 1.5:2.5:1, respectively.

are amorphous structures in nature. These peaks are confirmed according to the standard crystallographic database of silica nanoparticles with Card (no.47-0715) of the JCPDS (Joint Committee on Powder Diffraction Standards) (37,38).

Scanning Electron Microscopy (SEM) and Energy Dispersive X-Ray Spectroscopy (EDX) Analysis

The surface morphology of silica nanoparticles was explored by Scanning Electron Microscopy (SEM) analysis. From the SEM images, as shown in Figure 4, it is clearly illustrated that almost monodisperse, spherical, and uniform size of silica nanoparticles have been successfully prepared from the sol-gel synthesis process. The influence of different concentrations of TEOS on the particle size and size distribution of silica can be also analyzed from the SEM images. From Figures 4(a, d), it can be seen that the silica nanoparticles with the particle size distribution of 60-140 nm and the average particle size of 95±5.59 nm are produced from 1 mL of TEOS. When the amount of TEOS is increased to 2 mL during synthesis, comparatively larger particle sizes are found. The particle size of these silica nanoparticles ranging from 120 to 240 nm with

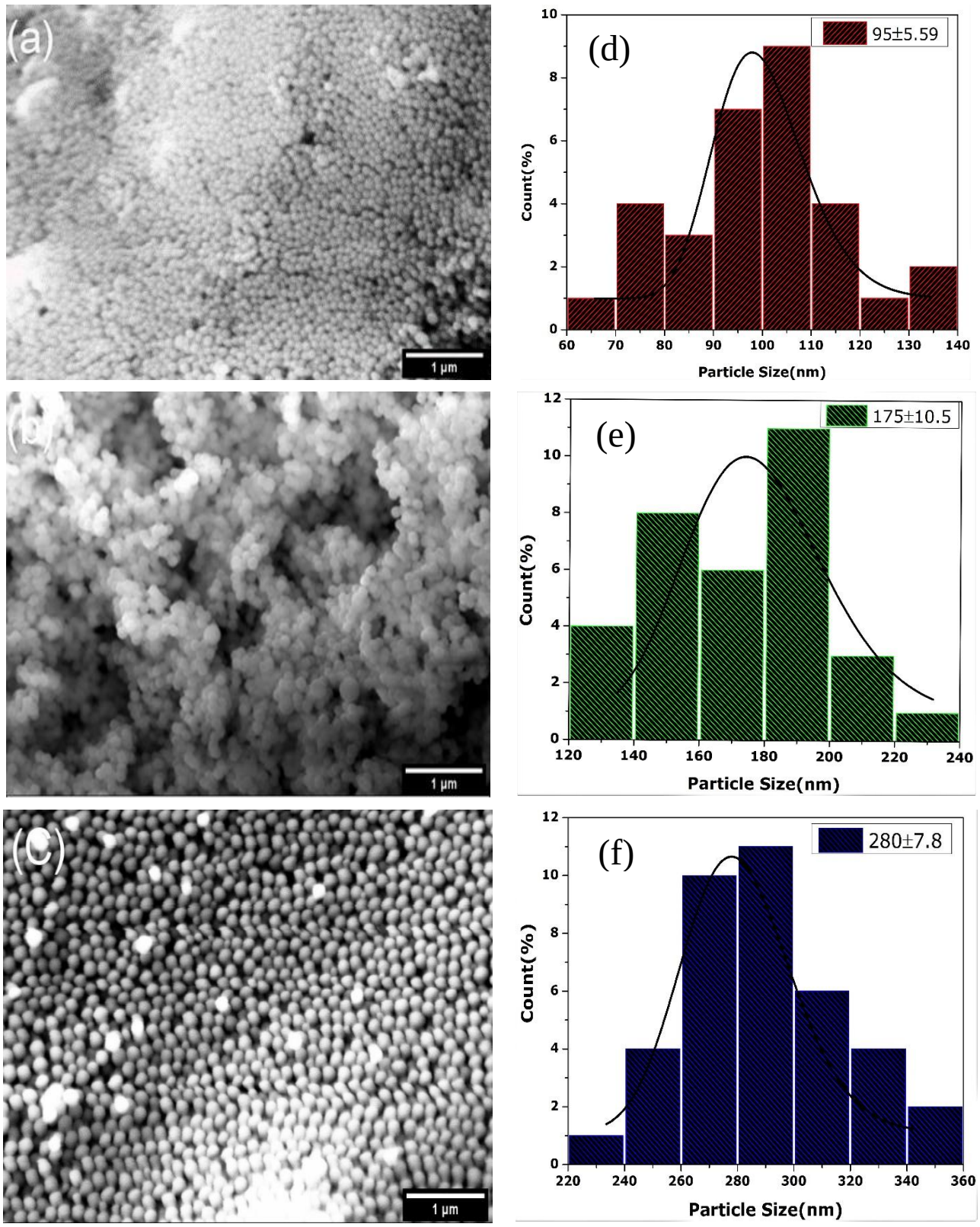

Figure 4: SEM images and size distribution histograms of Silica nanoparticles synthesized from volume ratios of TEOS: water: Ammonia =**S1 (a, d)** 1:5:2; **S2 (b, e)** 1:2.5:1; **S3 (c, f)** 1.5:2.5:1 respectively.

the average particle size of 175±10.5 nm has been shown in Figures 4(b, e). From a group of researchers, it has been studied that the concentration of TEOS is one of the key factors which determines the size of silica nanoparticles by controlling the concentration of primary particles present in the solution (23). Because of being at the early stage of supersaturated solution in the sol-gel process, nucleation will first take place which will induce the formation of a large number of primary particles within a short time. After this induction period, they rapidly aggregated to produce stable particles. Highly monodisperse and spherical nanoparticles can be obtained by implying that the stable particles formed during the induction period are sufficient to consume all primary particles nucleated after the induction period. That's why the particle sizes are directly influenced by the concentration of TEOS ~~(39)(40)~~ (39,40).

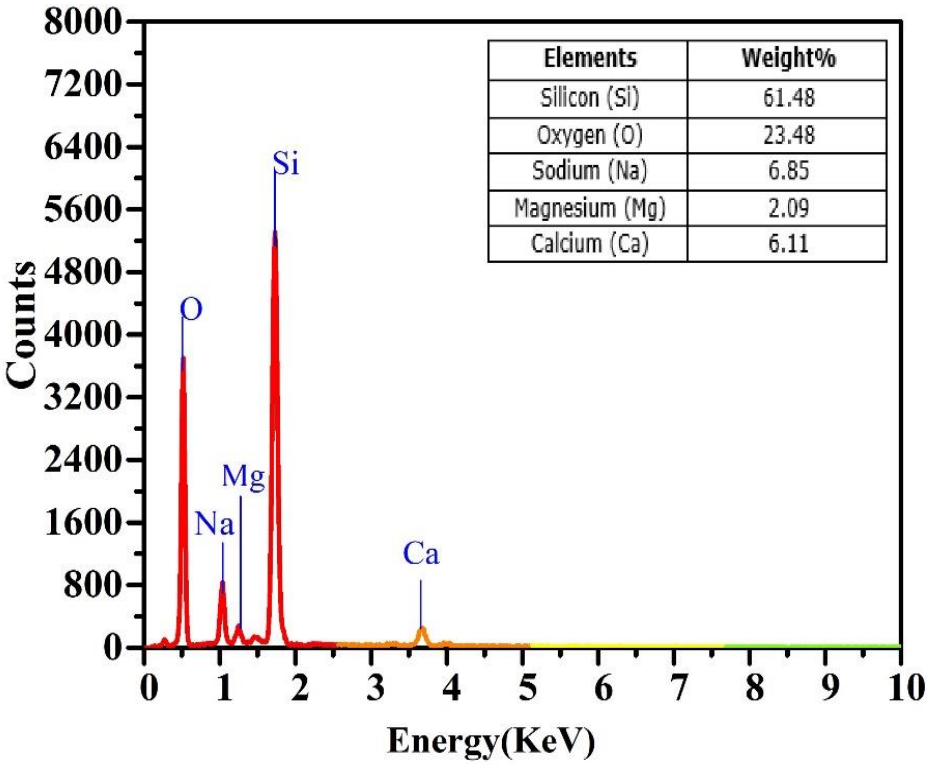

Figure 5: EDX spectrum of amorphous silica nanoparticles of S1 sample (average size of 95±5.59 nm and size distribution of 60-140 nm).

When the amount of TEOS is increased from 1 mL to 2 mL in the reaction vessel, the average size of silica particles is also increased from 95±5.59 nm to 175±10.5 nm. As the amount of TEOS is increased, both rate of hydrolysis and condensation reaction also increase predominantly. In consequence, due to the high hydrolysis reaction, a large number of the intermediates $[Si(OR)_{4-X}(OH)_X]$ will be rapidly increased to generate a supersaturation solution. After reaching that region, the consumption rate of intermediates through condensation reaction is also relatively fast. Thus, it probably shortens the nucleation period. Therefore, a

fewer number of nuclei will be formed and we get a bigger particle size at the end (23,41). From Figures 4(c, f), it can be seen that the bigger silica nanoparticles are produced from 3 mL of TEOS with size distribution ranging from 220 to 360 nm and the average particle size of 280±7.8 nm. The SEM image in Figure 4(a) shows that the size distribution of silica nanoparticles is somewhat narrower than in Figures 4(b) and 4(c). At low concentrations of TEOS, relatively smaller particle sizes and narrower size distribution are formed due to slow hydrolysis and condensation reaction rate. At this time the electrostatic repulsive force impedes the uncontrollable growth and aggregation among the particles and stabilizes them(42). As a result, the particle size distribution of the S1 sample is relatively narrower than S2 and S3 samples. To check the elemental chemical composition of silica nanoparticles, Energy Dispersive X-Ray Spectroscopy (EDX) analysis was performed in SEM mode. The EDX spectrum of S1 sample due to smaller particle size and narrower size distribution is shown in Figure 5. The outcome from the EDX analysis indicates that the synthesized silica nanoparticles contain 61.48 wt% of silicon and 23.48 wt% of oxygen. Some contaminants such as Sodium (Na), Magnesium (Mg), and Calcium (Ca) are also detected with a little percentage in the EDX spectrum which could originate during the fabrication process. This data verifies that the EDX result of the synthesized silica nanoparticles is consistent with the FT-IR results.

Ultraviolet-Visible Spectrophotometry (UV-Vis) analysis

Ultraviolet-Visible analysis was used to characterize the optical properties of silica nanoparticles prepared from different concentrations of TEOS. The optical absorption spectra of silica nanoparticles were measured by introducing them into thin films which were coated on glass slides by the spin coating technique. The UV-Visible spectral analysis was performed using a UV-Visible spectrophotometer between the wavelength range of 300-1100 nm. The optical absorbance spectra of silica nanoparticles with different amounts of TEOS are shown in Figure 6. From the graph, it can be analyzed that with a higher concentration of TEOS, the absorbance value of silica nanoparticles increases. Because the high concentration of TEOS speeds up the rate of hydrolysis and condensation reaction and thereby it produces a larger particle size (43). When the average particle size of silica nanoparticles is 95±5.59 nm for the S1 sample, the absorption coefficient (α) is found to 5.24×10^5 cm^{-1}. The absoption coefficients are gradually increased to 7.47×10^5 cm^{-1} and 9.98×10^5 cm^{-1} for S2 and S3 samples respectively due to the formation of larger particle sizes. The optical band gap can be calculated from the tauc's equation which gives the relationship between the absorption coefficient (α) and incident photon energy ($h\vartheta$) (44). The equation can be expressed as

$$(\alpha h\vartheta)^{1/n} = \beta(h\vartheta - E_g) \qquad (1)$$

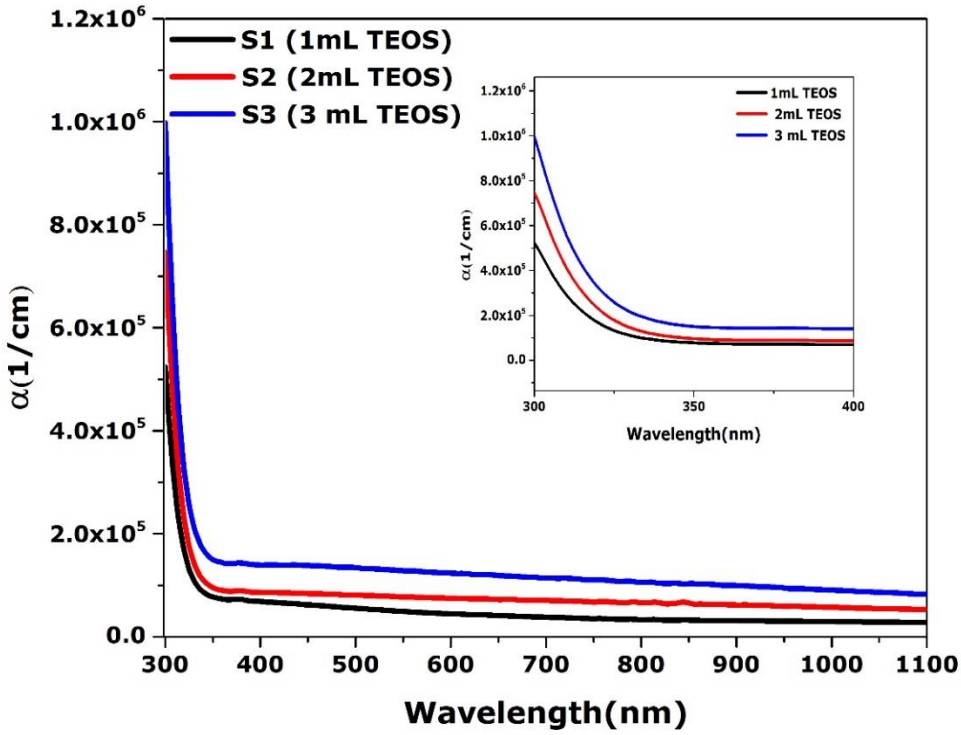

Figure 6: The absorbance spectra of silica nanoparticles prepared using different volume ratios of TEOS: water: Ammonia = **(S1)** 1:5:2 **(S2)** 1:2.5:1 **(S3)** 1.5:2.5:1, respectively.

Where, E_g is the band gap energy of the material, ϑ is the photon's frequency, α is the absorption coefficient, h is planck's constant, β is the band tailing parameter which depends on the disorder of the materials and n is the power factor of the optical transition mode that depends on the material's property. The power number (n) reveals ½ for direct allowed, 3/2 for direct forbidden, 2 for indirect allowed, and ≥3 for indirect forbidden transitions (45,46). Now the power factor n can be easily calculated from the equation

$$\frac{1}{n}\ln(\alpha h\vartheta) = \ln\beta + \ln(h\vartheta - E_g) \qquad (2)$$

The optical band gaps of the silica nanoparticles are obtained from the Tauc plot by plotting incident photon energy $h\vartheta$ in eV against $(\alpha h\vartheta)^2$.

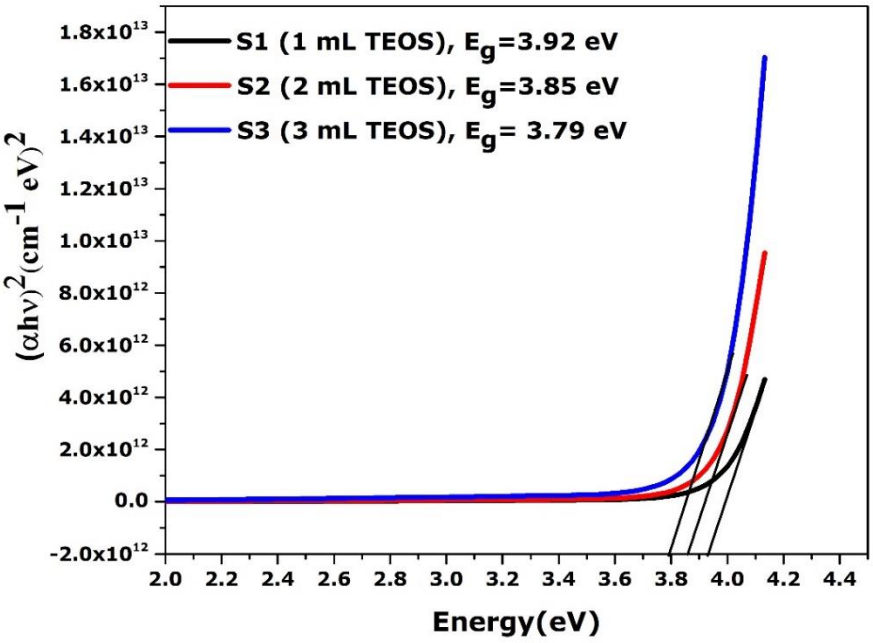

Figure 7: Determination of optical band gaps of Silica nanoparticles prepared from using different volume ratios of TEOS: water: ammonia = **(S1)** 1:5:2 **(S2)** 1:2.5:1 **(S3)** 1.5:2.5:1 respectively.

Figure 7 shows the optical band gaps of the samples S1, S2, and S3 are 3.92 eV, 3.85 eV, and 3.79 eV, respectively, which are found by extrapolating the intercept at $\alpha = 0$ in the Tauc plot**.** It is observed that the optical band gaps of silica nanoparticles continuously decrease with increasing the concentration of TEOS. This is because the particle sizes of silica are increased with increasing the concentration of TEOS whereas its dielectric function remains constant in the wavelength range of 300-1100 nm (43,46).

CONCLUSION

Silica nanoparticles were successfully synthesized from the hydrolysis and condensation reaction of TEOS in ethanol solution. During the fabrication process, TEOS was utilized as a precursor and ammonia as a catalyst. The chemical bonds in silica nanoparticles were noticed from FTIR analysis by confirming the different absorption peaks related to the Si-O-Si bonds. Furthermore, from the XRD spectrum, a broad diffused peak was discovered which asserted the amorphous structure of the silica nanoparticles. However, the spherical and uniform size of silica nanoparticles ranging from 95±5.59~280±7.8 nm were found from the different amounts of TEOS while keeping the other reaction parameters at a fixed condition. It was

discovered that the size of nanoparticles became larger when the concentration of TEOS was gradually increased. So, when using 1 mL of TEOS, spherical and amorphous silica nanoparticles with the average particle size of 95±5.59 nm and particle size distribution of 60-140 nm were produced. The particle size and size distribution became wider when using the higher concentration of TEOS. Hence, the average particle sizes of 175±10.5 and 280±7.8 nm and particle size distributions of 120-240 nm and 220-360 nm were found from 2 mL and 3mL of TEOS respectively. The variation in TEOS concentration also affects the optical absorbance of silica nanoparticles. Therefore, the optical absorbance of silica nanoparticles was increased with increasing the concentration of TEOS. Consequently, the optical bandgap of silica nanoparticles was reduced from 3.92 eV to 3.79 eV.

ACKNOWLEDGMENTS

The authors would like to express gratitude to the chemical synthesis laboratory at the institute of fuel research and development, BCSIR, Dhaka, Bangladesh for the research facilities.

REFERENCES

1. Jeelani PG, Mulay P, Venkat R, Ramalingam C. Multifaceted Application of Silica Nanoparticles. A Review. Silicon. 2020;12(6):1337–54. <DOI>
2. Karim AH, Ali A, Mezan S. Synthesis and Characterization of Silica Nanoparticle (Sio 2 Nps) Via Chemical Process. 2021;25(6):6211–8. <DOI>
3. Zhang W, Tu J, Long W, Lai W, Sheng Y, Guo T. Preparation of SiO2 anti-reflection coatings by sol-gel method. Energy Procedia [Internet]. 2017;130:72–6. Available from: <DOI>
4. Musigapong P, Briffa SM, Lynch I, Soontaranon S, Chanlek N, Valsami-Jones E. Silica nanoparticle synthesis and multi-method characterisation. Mater Sci Forum. 2019;947 MSF:82–90. <DOI>
5. Kim KIDO, Kim HEET. Formation of Silica Nanoparticles by Hydrolysis of TEOS Using a Mixed Semi-Batch / Batch Method. 2002;183–9.
6. Zhao S, Xu D, Ma H, Sun Z, Guan J. Controllable preparation and formation mechanism of monodispersed silica particles with binary sizes. J Colloid Interface Sci [Internet]. 2012;388(1):40–6. Available from: <DOI>
7. Gleiter H, Schimmel T, Hahn H. Nanostructured solids - From nano-glasses to quantum transistors. Nano Today [Internet]. 2014;9(1):17–68. Available from: <DOI>
8. Wang XD, Shen ZX, Sang T, Cheng X Bin, Li MF, Chen LY, et al. Preparation of spherical silica particles by Stöber process with high concentration of tetra-ethyl-orthosilicate. J Colloid Interface Sci [Internet]. 2010;341(1):23–9. Available from: <DOI>

9. Xu J, Ren D, Chen N, Li X, Ye Z, Ma S, et al. A facile cooling strategy for the preparation of silica nanoparticles with rough surface utilizing a modified Stöber system. Colloids Surfaces A Physicochem Eng Asp [Internet]. 2021;625(January):126845. Available from: <DOI>

10. Rahman IA, Padavettan V. Synthesis of Silica Nanoparticles by Sol-Gel : Size-Dependent Properties , Surface Modification , and Applications in Silica-Polymer Nanocomposites — A Review. 2012;2012. <DOI>

11. Huang Y, Pemberton JE. Synthesis of uniform, spherical sub-100nm silica particles using a conceptual modification of the classic LaMer model. Colloids Surfaces A Physicochem Eng Asp [Internet]. 2010;360(1–3):175–83. Available from: <DOI>

12. Rahman IA, Vejayakumaran P, Sipaut CS, Ismail J, Chee CK. Size-dependent physicochemical and optical properties of silica nanoparticles. Mater Chem Phys. 2009;114(1):328–32.<DOI>

13. Pe J, Liz-marza LM. Recent Progress on Silica Coating of Nanoparticles and Related Nanomaterials. 2010;36310:1182–95. <DOI>

14. Hyde EDER, Seyfaee A, Neville F, Moreno-atanasio R. Colloidal Silica Particle Synthesis and Future Industrial Manufacturing Pathways : A Review. 2016; <DOI>

15. Stanley R, Nesaraj a S. Effect of Surfactants on the Wet Chemical Synthesis of Silica Nanoparticles. 2014;(October 2013):9–21.<DOI>

16. Finnie KS, Bartlett JR, Barbé CJA, Kong L. Formation of silica nanoparticles in microemulsions. Langmuir. 2007;23(6):3017–24. <DOI>

17. Ren D, Xu J, Chen N, Ye Z, Li X, Chen Q, et al. Controlled synthesis of mesoporous silica nanoparticles with tunable architectures via oil-water microemulsion assembly process. Colloids Surfaces A Physicochem Eng Asp [Internet]. 2021;611(August):125773. Available from: <DOI>

18. Deng TS, Zhang QF, Zhang JY, Shen X, Zhu KT, Wu JL. One-step synthesis of highly monodisperse hybrid silica spheres in aqueous solution. J Colloid Interface Sci [Internet]. 2009;329(2):292–9. Available from: <DOI>

19. Dubey RS, Rajesh YBRD, More MA. Synthesis and Characterization of SiO2 Nanoparticles via Sol-gel Method for Industrial Applications. Mater Today Proc [Internet]. 2015;2(4–5):3575–9. Available from: <DOI>

20. Prabha S, Durgalakshmi D, Rajendran S, Lichtfouse E. Plant-derived silica nanoparticles and composites for biosensors, bioimaging, drug delivery and supercapacitors: a review. Environ Chem Lett [Internet]. 2021;19(2):1667–91. Available from: <DOI>

21. Zaky RR, Hessien MM, El-Midany AA, Khedr MH, Abdel-Aal EA, El-Barawy KA. Preparation of silica nanoparticles from semi-burned rice straw ash. Powder Technol. 2008;185(1):31–5. <DOI>

22. Stober WERNER. Controlled Growth of Monodisperse Silica Spheres in the Micron Size Range 1. 1968;69:62–9.

23. Bogush GH, Zukoski IV CF. Studies of the kinetics of the precipitation of uniform silica particles through the hydrolysis and condensation of silicon alkoxides. J Colloid Interface Sci. 1991;142(1):1–18.

24. Qasim M, Ananthaiah J, Dhara S, Paik P, Das D. Synthesis and Characterization of Ultra-Fine Colloidal Silica Nanoparticles. Adv Sci Eng Med. 2014;6(9):965–73.<DOI>

25. Meier M, Ungerer J, Klinge M, Nirschl H. Synthesis of nanometric silica particles via a

modi fi ed Stöber synthesis route. Colloids Surfaces A [Internet]. 2018;538(September 2017):559–64. Available from: <DOI>

26. Sreenivasa K, El-hami K, Kodaki T, Matsushige K. A novel method for synthesis of silica nanoparticles. 2005;289:125–31. <DOI>

27. Guo Q, Huang D, Kou X, Cao W, Li L, Ge L, et al. Synthesis of disperse amorphous SiO2 nanoparticles via sol–gel process. Ceram Int. 2017;43(1):192–6. <DOI>

28. Rahman IA, Vejayakumaran P, Sipaut CS, Ismail J, Bakar MA, Adnan R, et al. An optimized sol-gel synthesis of stable primary equivalent silica particles. Colloids Surfaces A Physicochem Eng Asp. 2007;294(1–3):102–10. <DOI>

29. Sung JY, Lee BRD. Structure and transmittance behavior of sol – gel silica nanoparticles synthesized using pH-stable alkanolamines. 2017;1–9. <DOI>

30. Gao GM, Zou HF, Liu DR, Miao LN, Ji GJ, Gan SC. Influence of surfactant surface coverage and aging time on physical properties of silica nanoparticles. Colloids Surfaces A Physicochem Eng Asp. 2009;350(1–3):33–7.<DOI>

31. Devi P, Vishal, Singla ML. Effect of surfactant concentration, solvents and particle size on Π-A isotherm of silica nanoparticles. Mater Lett [Internet]. 2013;107:107–10. Available from: <DOI>

32. Kim S, Kim H, Geon S, Kim W. Effect of electrolyte additives on sol-precipitated nano silica particles. 2004;30:171–5. <DOI>

33. Guo Q, Yang G, Huang D, Cao W, Ge L, Li L. Synthesis and characterization of spherical silica nanoparticles by modified Stöber process assisted by slow-hydrolysis catalyst. Colloid Polym Sci. 2018;296(2):379–84. <DOI>

34. Das S, Banerjee C, Kundu A, Dey P. Silica nanoparticles on front glass for efficiency enhancement in superstrate-type amorphous silicon solar cells. 415102.

35. Jiang X, Tang X, Tang L, Zhang B, Mao H. Synthesis and formation mechanism of amorphous silica particles via sol–gel process with tetraethylorthosilicate. Ceram Int [Internet]. 2019;45(6):7673–80. Available from: <DOI>

36. Yang G, Guo Q, Yang D, Peng P, Li J. Disperse ultrafine amorphous SiO 2 nanoparticles synthesized via precipitation and calcination. Colloids Surfaces A Physicochem Eng Asp [Internet]. 2019;568:445–54. Available from: <DOI>

37. Yang D, Yang G, Liang G, Guo Q, Li Y, Li J. High-surface-area disperse silica nanoparticles prepared via sol-gel method using L-lysine catalyst and methanol/water co-solvent. Colloids Surfaces A Physicochem Eng Asp [Internet]. 2021;610(July 2020):125700. Available from: <DOI>

38. Kim TG, An GS, Han JS, Hur JU, Park BG, Choi SC. Synthesis of size controlled spherical silica nanoparticles via sol-gel process within hydrophilic solvent. J Korean Ceram Soc. 2017;54(1):49–54. <DOI>

39. Ibrahim I a. M, Zikry a. a. F, Sharaf M a. Preparation of spherical silica nanoparticles: Stober silica. J Am Sci. 2010;6(11):985–9.

40. H GHB, Y MAT, IV CFZ. Preparation of Monodisperse Silica Particles: Control of Size and Mass Fraction. J Non Cryst Solids. 1988;104:95–106.

41. Chou K Sen, Chen CC. Preparation of monodispersed silica colloids using sol-gel method: COSOLVENT effect. Ceram Trans. 2005;166:57–67.

42. Giesche H. Synthesis of Monodispersed Silica Powders I . Particle Properties and

Reaction Kinetics. 1994;14:189–204.

43. Jamali N. Effect of Tetraethyl-Orthosilicate , 3-Aminopropyltriethoxysilane and Polyvinylpyrrolidone for synthesis of SiO 2 @ Ag core-shell nanoparticles prepared by chemical reduction method. 2021;1:31–8. <DOI>

44. Al-bataineh QM, Alsaad AM, Ahmad AA, Telfah A. Heliyon A novel optical model of the experimental transmission spectra of nanocomposite PVC-PS hybrid thin fi lms doped with silica nanoparticles. Heliyon [Internet]. 2020;6(June):e04177. Available from: <DOI>

45. Gupta P, Kumar K, Kumar N, Bal P, Yadav C, Hasan S. Effect of annealing temperature on a highly sensitive nickel oxide - based LPG sensor operated at room temperature. Appl Phys A [Internet]. 2021;127(4):1–15. Available from: <DOI>

46. Sankar S, Kaur N, Lee S, Kim Y.Rapid Sonochemical Synthesis of Spherical Silica Rapid Sonochemical Synthesis of Spherical Silica Nanoparticles Derived from Brown Rice Husk. Ceram Int [Internet]. 2018; Available from: <DOI>